JACS
JOURNAL OF THE AMERICAN CHEMICAL SOCIETY
Article
pubs.acs.org/JACS

Small Molecules Based on Benzo[1,2-b:4,5-b′]dithiophene Unit for High-Performance Solution-Processed Organic Solar Cells

Jiaoyan Zhou,[†,§] Xiangjian Wan,[†,§] Yongsheng Liu,[†] Yi Zuo,[†] Zhi Li,[†] Guangrui He,[†] Guankui Long,[†] Wang Ni,[†] Chenxi Li,[†] Xuncheng Su,[‡] and Yongsheng Chen*[,†]

[†]Key Laboratory for Functional Polymer Materials and Centre for Nanoscale Science and Technology, Institute of Polymer Chemistry, and [‡]State Key Laboratory of Elemento-Organic Chemistry, College of Chemistry, Nankai University, Tianjin 300071, China

Supporting Information

ABSTRACT: Small molecules, namely, $DCAO_3TBDT$ and DR_3TBDT, with 2-ethylhexoxy substituted BDT as the central building block and octyl cyanoacetate and 3-ethylrhodanine as different terminal units with the same linkage of dioctyltert-thiophene, have been designed and synthesized. The photovoltaic properties of these two molecules as donors and fullerene derivatives as the acceptors in bulk heterojunction solar cells are studied. Among them, DR_3TBDT shows excellent photovoltaic performance, and power conversion efficiency as high as 7.38% (certified 7.10%) under AM 1.5G irradiation (100 mW cm^{-2}) has been achieved using the simple solution spin-coating fabrication process, which is the highest efficiency reported to date for any small-molecule-based solar cells. The results demonstrate that structure fine turning could cause significant performance difference and with that the performance of solution-processed small-molecule solar cells can indeed be comparable with or even surpass their polymer counterparts.

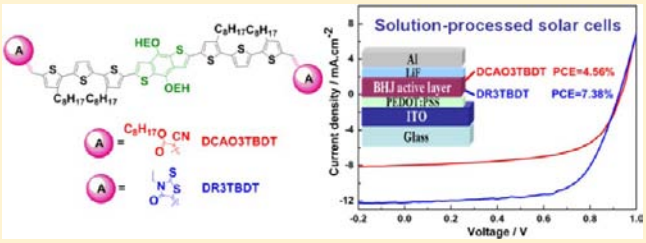

INTRODUCTION

Solution-processed organic solar cells (OSCs) are drawing more and more attention recently because of the potential as a competitive technology of green energy with the advantages of low cost, lightweight, and high mechanical flexibility.[1−5] With the significant improvements in active layer, device structure, and fabricating techniques, power conversion efficiencies (PCEs) over 8% have been achieved for polymer-based solar cells (PSCs) with the most promising bulk heterojunction (BHJ) architecture.[6−10] Meanwhile, solution-processed small-molecule-based solar cells (SMSCs) are emerging as a competitive alterative to their polymer counterparts due to some promising advantages, including well-defined structure thus less batch-to-batch variation,[11,12] versatile molecular structure, and easier band structure control.[13,14] Recently, prominent efficiencies with 6−7% have been achieved for small-molecule bulk heterojunction (SM BHJ) solar cells,[15−19] which is closing the performance gap with the best PSCs. However, SM BHJ solar cells have not been investigated as intensively as PSCs, and their overall performances are still behind those of their polymer counterparts. Furthermore, many techniques and lessons for polymer-based BHJ solar cells could be applied for SM BHJ devices.[4] Currently, the active materials, especially the donor materials are still the most important key factor for high PCEs of SMSC devices.[3,4] To address this issue, it is believed that several requirements should be considered collectively to design small molecules for high-performance and solution-processed SMSCs. These include (1) excellent film formation ability, (2) wide and efficient absorption, (3) matched energy levels with acceptors, (4) planar structure for high hole mobility, and (5) good solubility and chemical and thermal stability.[20] It is important to note that the design of small molecules with good film formation ability is a prerequisite for high-performance solution-processed BHJ devices, since it has been generally difficult for small molecules to form comparably good quality film as polymers, especially those molecules with relatively low molecular weights and rigid planar structures owing to their intrinsic aggregation.[21,22]

In our previous works, we have reported a series of linear acceptor−donor−acceptor (A-D-A) small molecules containing different cores such as thiophene,[16,23,24] dithieno[3,2-b:2′,3′-*d*]silole (DTS),[25] and benzo[1,2-b:4,5-b′]dithiophene (BDT)[26] with various terminal units, that is, alkyl cyanoacetate, 3-ethylrhodanine, and so forth. This design strategy could indeed efficiently solve the poor film quality problem for general small molecules owing to long enough conjugated backbone substituted with dispersed alkyl chains as used for the polymer cases. Meanwhile, taking the general advantages of small molecules, we find that those molecules exhibit high mobilities and wide absorptions with high coefficients, owing to the efficient conjugation in the backbone structure and intramolecule charge transfer (ICT) between the terminal acceptor units and the central donor building blocks. High PCEs with 5−6% have been achieved by employing them as the donors in BHJ devices with [6,6]-phenyl C_{61}-butyric acid methyl ester

Received: July 13, 2012
Published: September 18, 2012

dx.doi.org/10.1021/ja306865z | J. Am. Chem. Soc. 2012, 134, 16345−16351

($PC_{61}BM$) as the acceptor.[16,23,25,26] The results demonstrate that our strategy is effective, and it is expected that better PCEs could be achieved if careful molecule design can be carried out to address the above factors collectively by using more optimized building units.

Considering the relatively larger planar structure of benzo-[1,2-b:4,5-b′]dithiophene (BDT), its low highest occupied molecular orbital (HOMO) energy level, and proved high efficiencies in PSCs,[6,27] we have previously reported a small molecule named $DCAO_3T(BDT)_3T$ containing a none substituted BDT core and octyl cyanoacetate terminal with a PCE of 5.44%.[26] For $DCAO_3T(BDT)_3T$, we had to use a spacer unit of trioctylterthiophene to ensure its solubility and its film quality when using solution process for SM BHJ cells. Because of this, the synthesis of this particular compound is not efficient, and the route is long. Furthermore, though with a high open-circuit voltage (V_{oc}) of 0.93 V and fill factor (FF) of 59.9%, the device based on $DCAO_3T(BDT)_3T$ exhibited a relatively low short-circuit current (J_{sc}) of 9.77 mA cm^{-2} Later, we also found that incorporating a dye unit such as 3-ethylrhodanine as the end unit could greatly improve the light absorption ability, and thus, a high J_{sc} value could be achieved in the corresponding devices.[16] Logically, if taking advantages of these two results together, we could expect a higher performance for the easier-synthesis targeted compounds. Based on this, two molecules, namely, $DCAO_3TBDT$ and DR_3TBDT (Figure 1), with 2-ethylhexoxy substituted BDT block as the central building block and octyl cyanoacetate and 3-ethylrhodanine as the terminal unit, have been designed and synthesized. Their photovoltaic as well as other properties are studied and compared. Among them, DR_3TBDT shows excellent photovoltaic performance, and a PCE as high as 7.38% has been achieved using the simple solution spin-coating fabrication process.

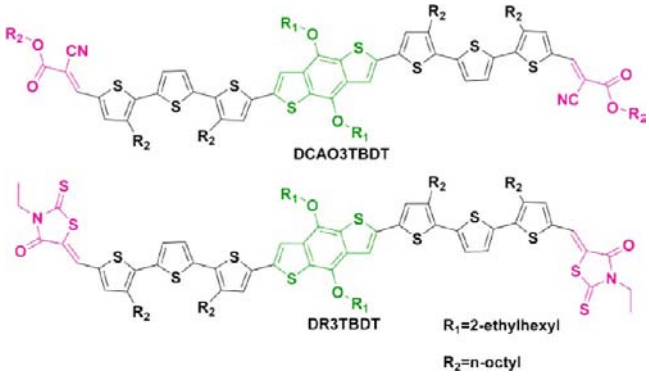

Figure 1. Chemical structures of the targeted molecules $DCAO_3TBDT$ and DR_3TBDT.

EXPERIMENTAL SECTION

Materials. All reactions and manipulations were carried out under argon atmosphere with the use of standard Schlenk techniques. $PC_{61}BM$ and $PC_{71}BM$ were purchased from American Dye Source, Inc., and PDMS (trimethylsiloxy terminated, M_r = 14 000) was purchased from Alfa Aesar. All the materials were used as received unless specified. Two important intermediates, 5-bromo-3,3-dioctyl-2,2′:5,2″-terthiophene-2-carbaldehyde(Br_3TCHO) (compound **1** in Scheme 1)[25] and 2,6-bis(trimethyltin)-4,8-bis(2-ethylhexoxy)benzo-[1,2-b:4,5-b′]dithiophene (BDT) (compound **2** in Scheme 1),[28] were prepared according to the literature.

Scheme 1. Synthesis Routes of $DCAO_3TBDT$ and DR_3TBDT[a]

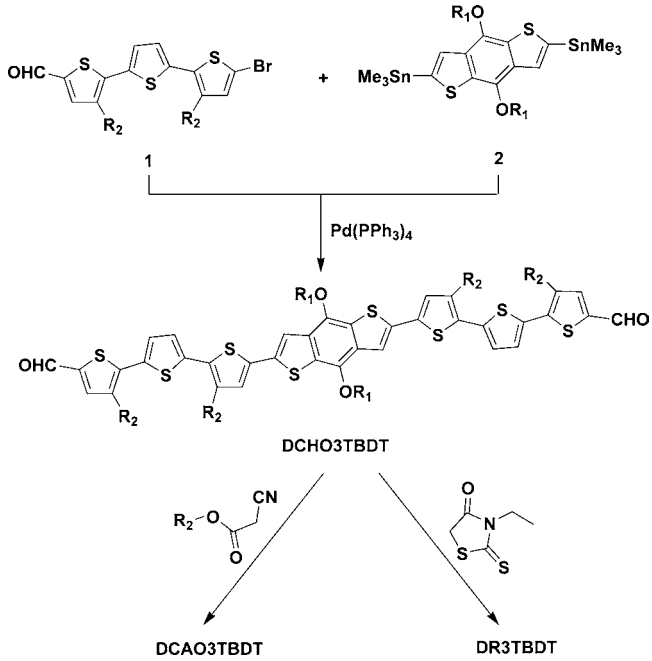

[a] R_1 = 2-ethylhexyl; R_2 = *n*-octyl.

$DCHO_3TBDT$. As shown in Scheme 1, a solution of **1** (1.67 g, 2.88 mmol) and **2** (1.06 g, 1.37 mmol) in toluene (70 mL) was degassed twice with argon followed by the addition of $Pd(PPh_3)_4$ (158 mg, 0.14 mmol). After being stirred at 100 °C for 48 h under argon, the reaction mixture was poured into water (100 mL) and extracted with CH_2Cl_2. The organic layer was washed with water and then dried over Na_2SO_4. After removal of solvent, the crude product was purified by column chromatography on silica gel using a mixture of dichloromethane and petroleum ether (1:1) as eluant to afford compound $DCHO_3TBDT$ (1.51 g, 73%) as a red solid. ^1H NMR (400 MHz, $CDCl_3$): δ 9.83 (s, 2H), 7.59 (s, 2H), 7.45 (m, 2H), 7.25 (s, 2H), 7.14 (m, 4H), 4.18 (d, 4H), 2.81 (m, 8H), 1.85 (m, 2H), 1.71 (m, 8H), 1.44 (m, 16H), 1.29 (m, 40H), 1.07 (t, 6H), 0.99 (br, 6H), 0.88 (m, 12H). ^{13}C NMR (100 MHz, $CDCl_3$): δ 182.52, 144.09, 141.16, 140.93, 140.36, 140.24, 139.07, 137.85, 136.09, 135.65, 134.75, 132.46, 130.19, 129.19, 128.31, 127.84, 126.31, 116.18, 40.69, 31.88, 30.52, 30.44, 30.31, 29.67, 29.53, 29.47, 29.31, 29.26, 23.88, 23.24, 22.69, 14.29, 14.13, 11.40. MS (MALDI-TOF): calcd. for $C_{84}H_{114}O_4S_8$ $[M]^+$, 1442.65; found, 1442.67.

$DCAO_3TBDT$. $DCHO_3TBDT$ (0.39 g, 0.27 mmol) was dissolved in a solution of dry $CHCl_3$ (60 mL); three drops of triethylamine and then octyl cyanoacetate (0.6 mL, 3.26 mmol) were added, and the resulting solution was stirred for 40 h under argon at room temperature. The reaction mixture was then extracted with CH_2Cl_2, washed with water, and dried over Na_2SO_4. After removal of solvent, it was purified by chromatography on silica gel using a mixture of dichloromethane and petroleum ether (3:2) as eluant to afford $DCAO_3TBDT$ as a black solid (0.31 g, 64% yield), mp 209−213 °C. ^1H NMR (400 MHz, $CDCl_3$): δ 8.20 (s, 2H), 7.59 (s, 2H), 7.46 (s, 2H), 7.31 (d, 2H), 7.16 (d, 2H), 7.15 (s, 2H), 4.29 (t, 4H), 4.19 (d, 4H), 2.82 (m, 8H), 1.85 (m, 2H), 1.73 (m, 16H), 1.45−1.29 (m, 72H), 1.07 (t, 6H), 0.99 (t, 6H), 0.88 (m, 18H). ^{13}C NMR (100 MHz, CDCl3): δ 163.10, 145.84, 144.09, 141.59, 141.18, 140.73, 140.49, 138.33, 136.05, 135.72, 134.33, 132.93, 132.46, 130.19, 129.19, 128.33, 128.18, 126.25, 116.19, 116.00, 97.70, 76.00, 66.55, 40.72, 31.88, 31.79, 30.46, 30.1, 29.77, 29.70, 29.59, 29.51, 29.33, 29.29, 29.21, 28.58, 25.82, 23.90, 23.26, 22.69, 22.66, 14.31, 14.12, 11.42. MS (MALDI-TOF): calcd for $C_{106}H_{148}N_2O_6S_8$ $[M]^+$, 1800.91; found,

dx.doi.org/10.1021/ja306865z | J. Am. Chem. Soc. 2012, 134, 16345−16351

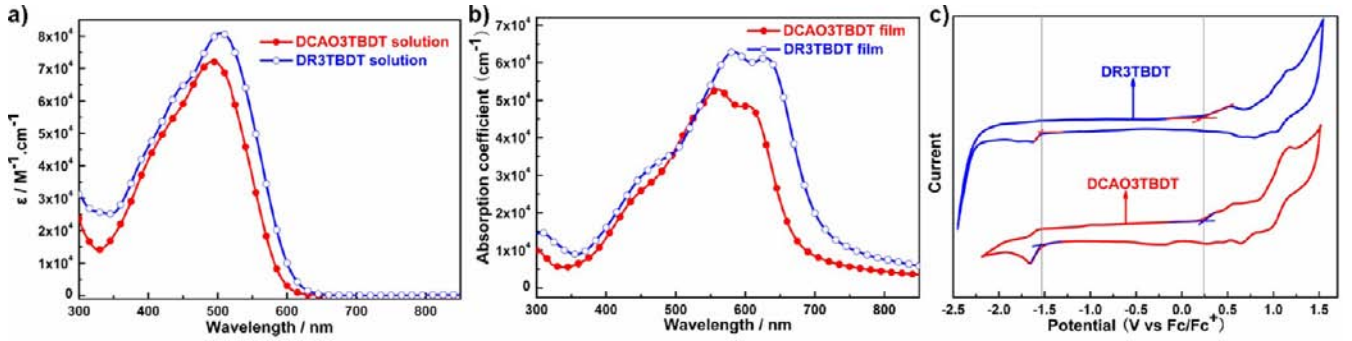

Figure 2. (a) UV−vis absorption spectra of $DCAO_3TBDT$ and DR_3TBDT solutions; (b) UV−vis absorption spectra of $DCAO_3TBDT$ and DR_3TBDT films; (c) cyclic voltammograms of $DCAO_3TBDT$ and DR_3TBDT in a dichloromethane solution of 0.1 mol L^{-1} Bu_4NPF_6 with a scan rate of 100 mV s^{-1}.

1800.91. Anal. calcd. for $C_{106}H_{148}N_2O_6S_8$: C, 70.62; H, 8.27; N, 1.55; found: C, 70.96; H, 8.62; N, 1.68.

DR_3TBDT. $DCHO_3TBDT$ (0.30 g, 0.21 mmol) was dissolved in a solution of dry $CHCl_3$ (50 mL); three drops of piperidine and then 3-ethylrhodanine (0.35 g, 2.1 mmol) were added, and the resulting solution was refluxed and stirred for 12 h under argon. The reaction mixture was then extracted with CH_2Cl_2, washed with water, and dried over Na_2SO_4. After removal of solvent, it was purified by chromatography on a silica gel column using $CHCl_3$ as eluant; the crude solid was recrystallized from hexane and $CHCl_3$ mixture four times to afford DR_3TBDTT as a black solid (290 mg, 80% yield), mp 232−237 °C. ^1H NMR (400 MHz, $CDCl_3$): δ 7.78 (s, 2H), 7.45 (s, 2H), 7.23 (br, 4H), 7.15 (br, 4H), 4.18−4.19 (br, 8H), 2.82 (d, 8H), 1.35−1.82 (m, 58H), 0.85−1.04 (m, 30H). ^{13}C NMR (100 MHz, $CDCl_3$): δ 192.05, 167.31, 144.10, 141.13, 139.45, 137.51, 137.32, 136.12, 135.89, 135.60, 135.28, 135.25, 134.81, 132.48, 130.36, 129.20, 127.33, 126.30, 124.88, 120.62, 116.22, 40.72, 39.93, 31.92, 31.85, 30.51, 30.31, 29.70, 29.69, 29.60, 29.50, 29.30, 23.95, 23.25, 22.70, 14.28, 14.11, 12.30, 11.42. MS (MALDI-FTICR): calcd. for $C_{94}H_{124}N_2O_4S_{12}$ $[M]^+$, 1729.62; found, 1730.62. Anal. calcd. for $C_{94}H_{124}N_2O_4S_{12}$: C, 65.23; H, 7.22; N, 1.62; found: C, 65.60; H, 7.06; N, 1.49.

Characterization. The ^1H and ^{13}C NMR spectra were recorded on a Bruker AV400 Spectrometer. High-resolution matrix-assisted laser desorption ionization (MALDI) mass spectra were collected with a Fourier transform-ion cyclotron resonance mass spectrometer instrument (Varian 7.0T FTICR-MS). The thermogravimetric analyses (TGA) was carried out on a NETZSCH STA 409PC instrument under purified nitrogen gas flow with a 10 °C min^{-1} heating rate. UV−vis spectra were obtained with a JASCO V-570 spectrophotometer. Cyclic voltammetry (CV) experiments were performed with a LK98B II microcomputer-based electrochemical analyzer. All CV measurements were carried out at room temperature with a conventional three-electrode configuration employing a glassy carbon electrode as the working electrode, a saturated calomel electrode (SCE) as the reference electrode, and a Pt wire as the counter electrode.[29] Dichloromethane was distilled from calcium hydride under dry nitrogen immediately prior to use. Tetrabutylammonium phosphorus hexafluoride (Bu_4NPF_6, 0.1 M) in dichloromethane was used as the supporting electrolyte, and the scan rate was 100 mV s^{-1}. The transmission electron microscopy (TEM) investigation was performed on a JEOL JEM2010FIF operated at 200 kV. Atomic force microscopy (AFM) investigation was performed using Bruker MultiMode 8 in "tapping" mode. The specimen for TEM measurement was prepared by spin-casting the blend solution on ITO/PEDOT−PSS substrate, floating the film on a water surface, and transferring to TEM grids. Incident photon to current efficiency (IPCE) values of the encapsulated devices was measured using a lock-in amplifier (SR810, Stanford Research Systems). The devices were illuminated by monochromatic light from a 150 W xenon lamp passing through an optical chopper and a monochromator. Photon flux was determined by a calibrated standard silicon photodiode.

Mobility measurements of $DCAO_3TBDT/PC_{61}BM$ (w/w, 1:0.5) and $DR_3TBDT/PC_{71}BM$ (w/w, 1:0.8) blend films with 0.2 mg mL^{-1} PDMS were done by a charge-only space-charge limited current (SCLC) method with the following diode structures: ITO/PEDOT−PSS/active layer/Au for hole and Al/active layer/Al for electron by taking current-voltage current in the range 0−7 V and fitting the results to a space-charge limited form.[30,31] The charge carrier mobilities were calculated using the SCLC model, where the SCLC is described by $J = 9\varepsilon_0\varepsilon_r\mu V^2/8L^3$, where J is the current density, L is the film thickness of the active layer, μ is the hole or electron mobility, ε_r is the relative dielectric constant of the transport medium, ε_0 is the permittivity of free space (8.85×10^{-12} F m^{-1}), V is the internal voltage in the device, and $V = V_{appl} - V_r - V_{bi}$, where V_{appl} is the applied voltage to the device, V_r is the voltage drop due to contact resistance and series resistance across the electrodes, and V_{bi} is the built-in voltage due to the relative work function difference of the two electrodes.

Solar Cell Fabrication and Testing. The devices were fabricated with a conventional structure of glass/ITO/PEDOT−PSS/donor−acceptor/LiF/Al using a solution process. The ITO-coated glass substrates were cleaned by ultrasonic treatment in detergent, deionized water, acetone, and isopropyl alcohol under ultrasonication for 15 min each and subsequently dried by a nitrogen blow. A thin layer (~40 nm) of PEDOT−PSS (Clevios P VP AI 4083, filtered at 0.45 μm) was spin-coated at 3000 rpm onto the ITO surface. After being baked at 150 °C for 20 min, the substrates were transferred into an argon-filled glovebox. Subsequently, the active layer (~100 nm) was spin-coated from donor (8 mg/mL)−acceptor blend chloroform solutions with different ratios at 1700 rpm. For the devices with PDMS additive, PDMS with desired amounts was added in the active material blend chloroform solutions and stirred for 2 h before spin-coating. Finally, a 0.8 nm LiF and 80 nm Al layer were deposited on the active layer under high vacuum ($<2 \times 10^{-4}$ Pa). The effective area of each cell was ~4 mm^2 defined by the mask. The current density−voltage (J−V) curves of photovoltaic devices were obtained by a Keithley 2400 source-measure unit. The photocurrent was measured under illumination simulated 100 mW cm^{-2} AM1.5G irradiation using an Oriel 96000 solar simulator, calibrated with a standard Si solar cell.

RESULTS AND DISCUSSION

Synthesis and Thermal Property. Figure 1 shows the chemical structures of these two molecules terminated with octyl cyanoacetate ($DCAO_3TBDT$) and 3-ethylrhodanine (DR_3TBDT). The synthesis routes of the two target molecules are depicted in Scheme 1. By using the 2-ethylhexoxy substituted BDT central building block for better solubility, we can select the easier-synthesized dioctyltertthiophene obtained via a simple Grignard reaction[25] as the spacer instead of trioctylterthiophene in our previous compound $DCAO_3T(BDT)_3T$, since the synthesis of the trioctylterthiophene block

Table 1. Optical and Electrochemical Data of Compounds $DCAO_3TBDT$ and DR_3TBDT

compd	λ_{max} solution (nm)	ε solution (M^{-1} cm^{-1})	λ_{max} film (nm)	ε film (cm^{-1})	(E_g^{opt}) film (eV)	E_g^{cv} (eV)	HOMO (eV)	LUMO (eV)
$DCAO_3TBDT$	494	7.2×10^4	560	5.3×10^4	1.84	1.80	−5.04	−3.24
DR_3TBDT	508	8.1×10^4	583	6.3×10^4	1.74	1.75	−5.02	−3.27

is rather tedious.[26] The targeted molecules were then prepared by the Knoevenagel condensation of $DCHO_3TBDT$ with octyl cyanoacetate or 3-ethylrhodanine, respectively. Obviously, the route for this synthesis is much easier and more efficient than the previous method and offers more possibility to have a more diversified pool of products for future studies. Both products are rather soluble in common organic solvents and exhibited good thermal stability up to 320 °C under a N_2 atmosphere (Supporting Information, Figure S1).

Optical Absorption and Electrochemical Properties. The solution and thin-film optical absorption spectra of $DCAO_3TBDT$ and DR_3TBDT were presented in Figure 2a, b. $DCAO_3TBDT$ in diluted chloroform solution shows an absorption peak at 494 nm and a maximal coefficient of 7.2×10^4 M^{-1} cm^{-1}. After replacing the octyl cyanoacetate terminal with 3-ethylrhodanine, the DR_3TBDT solution presents a bathochromic absorption peak at 508 nm, with a higher maximal coefficient of 8.1×10^4 M^{-1} cm^{-1}. At the solid state, the $DCAO_3TBDT$ film displays a red-shifted λ_{max} at 560 nm with a maximal coefficient of 5.3×10^4 cm^{-1}. The DR_3TBDT film shows a broader absorption from 350 to 800 nm and a red-shifted absorption peak at 583 nm with the maximal coefficient increasing to 6.3×10^4 cm^{-1} and also a vibronic shoulder at 640 nm, indicating an effective $\pi-\pi$ packing between the molecule backbones at the solid state.[32,33] It is obvious that the introduction of the rhodanine dye end unit could effectively lower the band gap and improve absorption coefficient as expected, which is similar to the rhodanine effect observed in our previous work.[16] The optical band gaps of $DCAO_3TBDT$ and DR_3TBDT are estimated to be 1.84 and 1.74 eV, respectively. Cyclic voltammetry (CV) was used to investigate the electrochemical property of $DCAO_3TBDT$ and DR_3TBDT. As shown in Figure 2c, the energy levels of HOMO and lowest unoccupied molecular orbital (LUMO), which are −5.04 and −3.24 eV for $DCAO_3TBDT$ and −5.02 and −3.27 eV for DR_3TBDT, were calculated from the onset oxidation and reduction potential. The electrochemical band gaps of $DCAO_3TBDT$ and DR_3TBDT are estimated to be 1.80 and 1.75 eV, respectively, which is consistent with the optical band gaps. So, compound DR_3TBDT exhibits a slightly lower band gap. Some important optical and electrochemistry data were displayed in Table 1.

Photovoltaic Properties. With the desired good solubility and high efficient solar light absorption, OSC devices based on these two small molecules were fabricated and tested under the illumination of AM 1.5G, 100 mW cm^{-2} for solar cell applications. Following our conventional practice for these small molecules using solution process,[23,25] the active layers were spin-coated from their chloroform solutions. The best $J-V$ curves are reported in Figure 3a, and the corresponding photovoltaic performance is summarized in Table 2. With the optimized weight ratio of $DCAO_3TBDT$ to $PC_{61}BM$ at 1:0.5, a best but moderate PCE of 4.56% was obtained, with a short-circuit current (J_{sc}) of 8.00 mA cm^{-2}, an open-circuit voltage (V_{oc}) of 0.95 V, and a fill factor (FF) of 60.0%. In contrast, the devices based on DR_3TBDT and $PC_{61}BM$ (1:0.8, w/w) received an impressive PCE of 6.38%, with a V_{oc} of 0.91 V

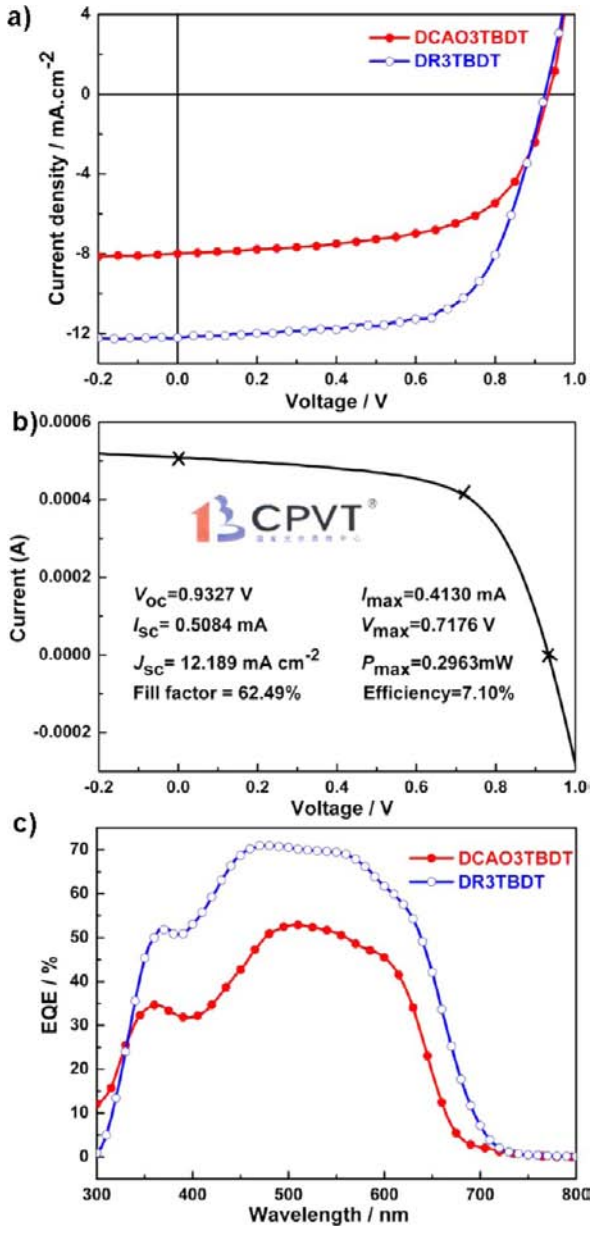

Figure 3. (a) $J-V$ curves of solar cells with an active layer composed of $DCAO_3TBDT/PC_{61}BM$ (1:0.5, w/w) and $DR_3TBDT/PC_{71}BM$ (1:0.8, w/w) with 0.2 mg mL^{-1} PDMS; (b) the certified performance of a device based on $DR_3TBDT/PC_{71}BM$ with 0.2 mg mL^{-1} PDMS; (c) EQE plots of solar cells with an active layer composed of $DCAO_3TBDT$/PC61BM (1:0.5, w/w) and $DR_3TBDT/PC_{71}BM$ (1:0.8, w/w) with 0.2 mg mL^{-1} PDMS.

and a FF of 65.0%, and a significantly higher J_{sc} of 10.78 mA cm^{-2} due to its better light absorption. The active layers were further investigated by using $PC_{71}BM$, which has a higher absorption coefficient in visible range,[34] as the electron acceptor. Interestingly, the PCE of devices based on $DCAO_3TBDT$ and $PC_{71}BM$ decreased sharply to 2.09% with a drop of J_{sc} to 3.74 mA cm^{-2}. However, the active layer with

dx.doi.org/10.1021/ja306865z | J. Am. Chem. Soc. 2012, 134, 16345−16351

Table 2. Device Performance Parameters for BHJ Solar Cells Based on $DCAO_3TBDT$ and DR_3TBDT

active layer	ratio	V_{oc}(V)	J_{sc} (mA cm^{-2})	FF (%)	PCE (%)
$DCAO_3TBDT$/$PC_{61}BM$	1:0.5	0.95	8.00	60.0	4.56
$DCAO_3TBDT$/$PC_{71}BM$	1:0.5	0.93	3.74	60.1	2.09
$DCAO_3TBDT$/$PC_{61}BM$[a]	1:0.5	0.94	6.60	60.9	3.78
$DR_3TBDT/PC_{61}BM$	1:0.8	0.91	10.78	65.0	6.38
$DR_3TBDT/PC_{71}BM$	1:0.8	0.93	11.40	65.3	6.92
$DR_3TBDT/PC_{71}BM$[a]	1:0.8	0.93	12.21	65.0	7.38[b]

[a]PDMS (0.2 mg mL^{-1}) was added to the active materials solution. [b]The average PCE is 7.18%, see the text.

DR_3TBDT and $PC_{71}BM$ yielded an increased PCE of 6.92% and an improved J_{sc} of 11.40 mA cm^{-2}. The contrary impact caused by the acceptors is probably due to the different morphology change that will be discussed below. Then, the devices using the blend of DR_3TBDT and $PC_{71}BM$ were intensively studied. During the devices optimization, it was found that the performance of DR_3TBDT could be further improved by adding a small amount of PDMS in the active layer.[35] With the addition of 0.2 mg mL^{-1} PDMS, the devices yield the best PCE of 7.38%, with J_{sc} of 12.21 mA cm^{-2}, V_{oc} of 0.93 V, and FF of 65.0%, which is the highest efficiency reported to date for any small-molecule-based solar cells. The average PCE is 7.18% for over a hundred devices under this optimized condition. The device performance was also certified after encapsulation with UV epoxy at the National Center of Supervision & Inspection on Solar Photovoltaic Products Quality of China (CPVT). A certificated PCE of 7.10% was obtained by the device based on DR_3TBDT (see Figure 3b), which has ~0.28% PCE degradation compared with that at our lab. We also used PDMS as the additive in the active layer of $DCAO_3TBDT$ and $PC_{61}BM$; however, no clear improvement was observed.

The external quantum efficiency (EQE) spectra of the optimized devices based on $DCAO_3TBDT$ and DR_3TBDT are shown in Figure 3c. The EQE curve of $DR_3TBDT/PC_{71}BM$ (w/w, 1:0.8) with 0.2 mg mL^{-1} PDMS exhibits efficient photoconversion efficiency from 320 to 700 nm, with the highest EQE value reaching 71% at 470 nm. The calculated J_{sc} integrated from the EQE for DR_3TBDTT is 11.50 mA cm^{-2} with around 5% mismatch compared to the J_{sc} from $J-V$ measurement. In comparison, the EQE value of the device based on $DCAO_3TBDT$ is below 50%, and it shows relatively narrower EQE response than that of DR_3TBDT, which results in a lower J_{sc} value in the $DCAO_3TBDT$-based device. These results are echoing the results of their UV absorption and prove that the incorporation of a rhodanine dye unit could indeed improve significantly the photoconversion efficiency and broaden the response range.

To understand the sharp difference in solar cell performance of these two compounds, transmission electron microscopy (TEM) (Figure 4) and atomic force microscopy (AFM) (Figure 5) were used to investigate their morphology of the blend films thoroughly. The TEM images indicate that the dissatisfactory solar cell performance of $DCAO_3TBDT$ is at least in some degree relevant to the no-optimized morphology of the blend film with $PC_{61}BM$ (Figure 4a), whose domain size is as large as 80 nm. Furthermore, when $PC_{71}BM$ was mixed with $DCAO_3TBDT$ (Figure 4b), the domain size even became larger than 100 nm, which should lead to even less efficient exciton separation, charge transport, and thus lower J_{sc}.[28] Adding PDMS for $DCAO_3TBDT$ does not seem to have much impact on the morphology as shown in Figure 4c. From AFM imagines (Figure 5a, b), it is found that the root-mean-square (rms) roughness of the $DCAO_3TBDT/PC_{61}BM$ blend film

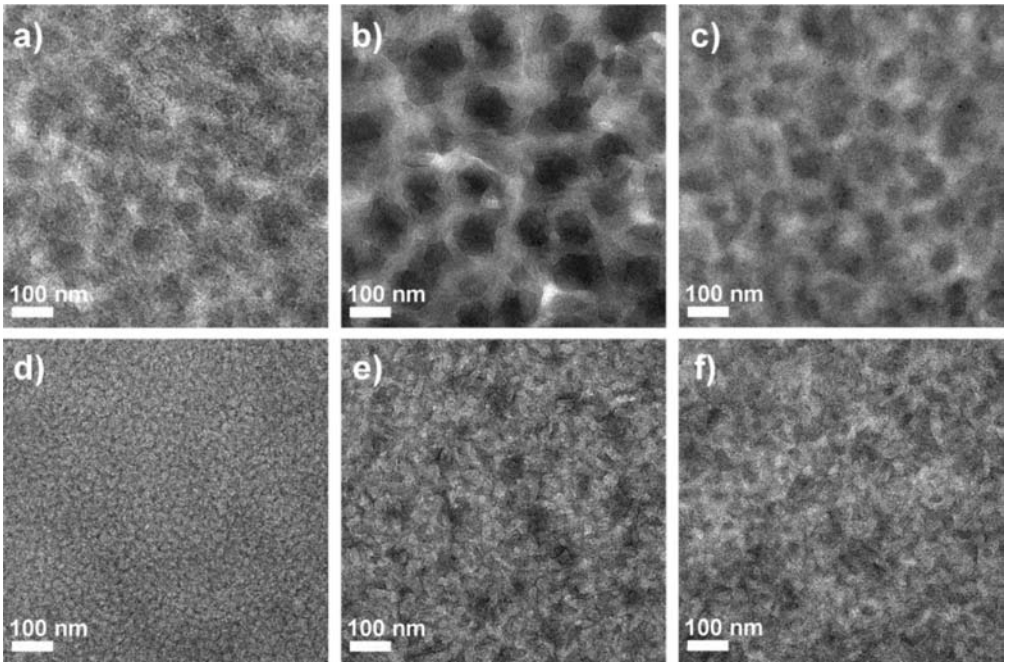

Figure 4. TEM images of the active layers with (a) DCAO3TBDT/$PC_{61}BM$ (1:0.5, w/w), (b) DCAO3TBDT/$PC_{71}BM$ (1:0.5, w/w), (c) DCAO3TBDT/$PC_{61}BM$ (1:0.5, w/w) with 0.2 mg mL^{-1} PDMS, (d) DR3TBDT/$PC_{61}BM$ (1:0.8, w/w), (e) DR3TBDT/$PC_{71}BM$ (1:0.8, w/w), and (f) DR3TBDT/$PC_{71}BM$ (1:0.8, w/w) with 0.2 mg mL^{-1} PDMS.

dx.doi.org/10.1021/ja306865z | J. Am. Chem. Soc. 2012, 134, 16345−16351

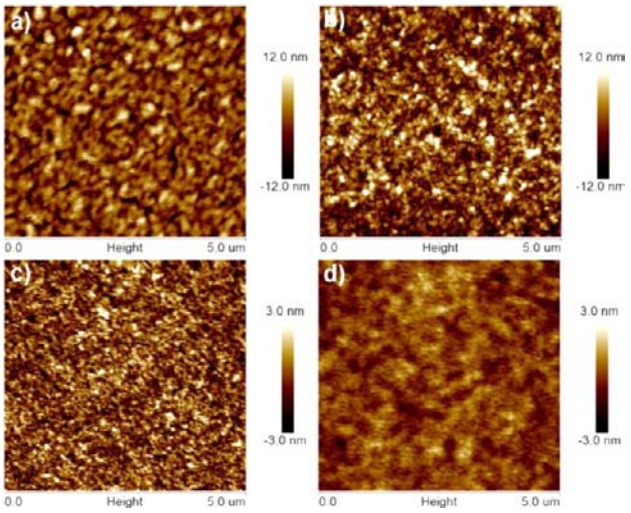

Figure 5. Tapping-mode AFM height images of the active layers with (a) $DCAO_3TBDT/PC_{61}BM$ (1:0.5, w/w), (b) $DCAO_3TBDT/PC_{61}BM$ (1:0.5, w/w) with 0.2 mg mL^{-1} PDMS, (c) $DR_3TBDT/PC_{71}BM$ (1:0.8, w/w), and (d) $DR_3TBDT/PC_{71}BM$ (1:0.8, w/w) with 0.2 mg mL^{-1} PDMS.

increases slightly from 3.40 to 4.38 nm with PDMS additive. The slight enhancement of roughness of the blend film indicates that addition of PDMS led to less evenly distributed morphological features than that of film without PDMS, which attributed the PCE slight difference of $DCAO_3TBDT/PC61BM$ with and without PDMS. Gratefully, TEM and AFM images of DR_3TBDT with $PC_{61}BM$ or $PC_{71}BM$ (Figures 4d–f and 5c, d) all show much better morphology than that for $DCAO_3TBDT$, and all exhibited rather uniform and even distributed domains (20–30 nm).[36] While it needs a more comprehensive study to understand, this significant difference in the morphology for these two compounds may be due to the increased miscibility of DR_3TBDT with PCBM compounds after shortening the length of the terminal unit from octyl cyanoacetate to 3-ethylrhodanine.[28] With the addition of small amount of PDMS (Figure 4f), the film forms evener continuous interpenetrating networks, and thus, it benefits to the exciton separation and charge transport,[36−38] which is consistent with the AFM results (Figure 5c, d). Different from that of $DCAO_3TBDT/PC_{61}BM$ blend film, the roughness of $DR_3TBDT/PC_{71}BM$ blend film decreases from 1.06 to 0.58 nm with PDMS additive, which could lead to more evenly distributed morphological features than that of film without PDMS. The great differences in the morphology of $DCAO_3TBDT$ and DR_3TBDT indicate that fine turning of the targeted molecular structure is critical to have the desired morphology in the solid state with acceptor and optimized solar cell performance.[3]

The mobilities of the optimized blend of $DCAO_3TBDT/PC_{61}BM$ and $DR_3TBDTT/PC_{71}BM$ were measured by the charge-only SCLC method (Supporting Information,Figures S7–S9). The $DCAO_3TBDT$ device without using PDMS presents a less matched hole and electron mobility of 1.38×10^{-4} cm^2 V^{-1} s^{-1} and 5.50×10^{-4} cm^2 V^{-1} s^{-1}, respectively. No clear improvement was observed when using PDMS for this compound. In contrary, the device of $DR_3TBDT/PC_{71}BM$ with the PDMS additive shows a much better balanced hole and electron mobility of 2.47×10^{-4} cm^2 V^{-1} s^{-1} and 3.13×10^{-4} cm^2 V^{-1} s^{-1}, respectively, which is consistent with the better performance of devices. Without the additive, while the device still shows good balanced hole and electron mobilities of 1.76×10^{-4} cm^2 V^{-1} s^{-1} and 1.01×10^{-4} cm^2 V^{-1} s^{-1}, respectively, both values are lower than those of the devices with PDMS additive. The enhancement of the hole and electron mobilities with PDMS additive indicates that an evener continuous interpenetrating network in the active film is formed, which is beneficial to the exciton separation and charge transport.[31]

CONCLUSION

In summary, two small molecules DR_3TBDTT and $DCAO_3TBDT$ with the A-D-A structure and BDT as the central building block have been designed and synthesized. The introduction of 3-ethylrhodanine terminal to the A-D-A structure improves solar light absorption significantly, and the solar cell devices based on the corresponding compound DR_3TBDT possesses much higher J_{sc} compared to that of the octyl cyanoacetate terminated compound $DCAO_3TBDT$. An impressive PCE of 7.38% was obtained from the DR_3TBDT-based solar cells, which is the highest for any small-molecule-based solar cell. The result is also comparable with that of the highest performance polymer-based solar cells, which demonstrates that promising and higher OSC performance for SM BHJ could indeed be achieved through rational molecule design and device fabrication controlling.

ASSOCIATED CONTENT

Supporting Information

TGA, other detailed photovoltaic data with different donor/acceptor ratios, and charge-only mobilities of $DCAO_3TBDT$ and DR_3TBDT. This material is available free of charge via the Internet at http://pubs.acs.org.

AUTHOR INFORMATION

Corresponding Author

yschen99@nankai.edu.cn

Author Contributions

§These authors contributed equally to this work.

Notes

The authors declare no competing financial interest.

ACKNOWLEDGMENTS

The authors gratefully acknowledge financial support from the MoST (grants 2011DFB50300 and 2012CB933401) and NSFC (grants 50933003, 50903044, and 21073101).

REFERENCES

(1) Thompson, B. C.; Frechet, J. M. *Angew. Chem., Int. Ed.* **2008**, *45*, 58–77.
(2) Zhou, H. X.; Yang, L. Q.; You, W. *Macromolecules* **2012**, *45*, 607–632.
(3) Mishra, A.; Bäuerle, P. *Angew. Chem., Int. Ed.* **2011**, *51*, 2020–2067.
(4) Lin, Y. Z.; Li, Y. F.; Zhan, X. W. *Chem. Soc. Rev.* **2012**, *41*, 4245–4272.
(5) Cheng, Y. J.; Yang, S. H.; Hsu, C. S. *Chem. Rev.* **2009**, *109*, 5868–5923.
(6) He, Z. C.; Zhong, C. M.; Huang, X.; Wong, W. Y.; Wu, H. B.; Chen, L. W.; Su, S. J.; Cao, Y. *Adv. Mater.* **2011**, *23*, 4636–4643.
(7) Small, C. E.; Chen, S.; Subbiah, J.; Amb, C. M.; Tsang, S. W.; Lai, T. H.; Reynolds, J. R.; So, F. *Nat. Photonics* **2012**, *6*, 115–120.

(8) Dou, L. T.; You, J. B.; Yang, J.; Chen, C.-C.; He, Y. J.; Murase, S.; Moriarty, T.; Emery, K.; Li, G.; Yang, Y. *Nat. Photonics* **2012**, *6*, 180−185.
(9) Li, X. H.; Choy, W. C. H.; Huo, L. J.; Xie, F. X.; Sha, W. E. I.; Ding, B. F.; Guo, X.; Li, Y. F.; Hou, J. H.; You, J. B.; Yang, Y. *Adv. Mater.* **2012**, *24*, 3046−3052.
(10) Chen, S.; Small, C. E.; Amb, C. M.; Subbiah, J.; Lai, T. H.; Tsang, S. W.; Manders, J. R.; Reynolds, J. R.; So, F. *Adv. Energy Mater.* **2012**, DOI: 10.1002/aenm.201200184.
(11) Shang, H. X.; Fan, H. J.; Liu, Y.; Hu, W. P.; Li, Y. F.; Zhan, X. W. *Adv. Mater.* **2011**, *23*, 1554−1557.
(12) Loser, S.; Bruns, C. J.; Miyauchi, H.; Ortiz, R. P.; Facchetti, A.; Stupp, S. I.; Marks, T. J. *J. Am. Chem. Soc.* **2011**, *133*, 8142−8145.
(13) Welch, G. C.; Perez, L. A.; Hoven, C. V.; Zhang, Y.; Dang, X. D.; Sharenko, A.; Toney, M. F.; Kramer, E. J.; Nguyen, T.-Q.; Bazan, G. C. *J. Mater. Chem.* **2011**, *21*, 12700−12709.
(14) Demeter, D.; Rousseau, T.; Leriche, P.; Cauchy, T.; Po, R.; Roncali, J. *Adv. Funct. Mater.* **2011**, *21*, 4379−4387.
(15) Steinmann, V.; Kronenberg, N. M.; Lenze, M. R.; Graf, S. M.; Hertel, D.; Meerholz, K.; Buerckstuemmer, H.; Tulyakova, E. V.; Wuerthner, F. *Adv. Energy Mater.* **2011**, *1*, 888−893.
(16) Li, Z.; He, G.; Wan, X.; Liu, Y.; Zhou, J.; Long, G.; Zuo, Y.; Zhang, M.; Chen, Y. *Adv. Energy Mater.* **2011**, *2*, 74−77.
(17) Sun, Y. M.; Welch, G. C.; Leong, W. L.; Takacs, C. J.; Bazan, G. C.; Heeger, A. J. *Nat. Mater.* **2012**, *11*, 44−48.
(18) Poll, T. S.; Love, J. A.; Nguyen, T.-Q.; Bazan, G. C. *Adv. Mater.* **2012**, *24*, 3646−3649.
(19) Fitzner, R.; Mena-Osteritz, E.; Mishra, A.; Schulz, G.; Reinold, E.; Weil, M.; Körner, C.; Ziehlke, H.; Elschner, C.; Leo, K.; Riede, M.; Pfeiffer, M.; Uhrich, C.; Bäuerle, P. *J. Am. Chem. Soc.* **2012**, *134*, 11064−11067.
(20) Li, Y. F. *Acc. Chem. Res.* **2012**, *45*, 723−733.
(21) Beaujuge, P. M.; Frechet, J. M. *J. Am. Chem. Soc.* **2011**, *133*, 20009−20029.
(22) Walker, B.; Kim, C.; Nguyen, T.-Q. *Chem. Mater.* **2011**, *23*, 470−482.
(23) Liu, Y.; Wan, X.; Wang, F.; Zhou, J.; Long, G.; Tian, J.; You, J.; Yang, Y.; Chen, Y. *Adv. Energy Mater.* **2011**, *1*, 771−775.
(24) He, G.; Li, Z.; Wan, X.; Liu, Y.; Zhou, J.; Long, G.; Zhang, M.; Chen, Y. *J. Mater. Chem.* **2012**, *22*, 9173−9180.
(25) Zhou, J.; Wan, X.; Liu, Y.; Long, G.; Wang, F.; Li, Z.; Zuo, Y.; Li, C.; Chen, Y. *Chem. Mater.* **2011**, *23*, 4666−4668.
(26) Liu, Y.; Wan, X.; Wang, F.; Zhou, J.; Long, G.; Tian, J.; Chen, Y. *Adv. Mater.* **2011**, *23*, 5387−5391.
(27) Chen, H. Y.; Hou, J. H.; Zhang, S. Q.; Liang, Y. Y.; Yang, G. W.; Yang, Y.; Yu, L. P.; Wu, Y.; Li, G. *Nat. Photonics* **2009**, *3*, 649−653.
(28) Liang, Y. Y.; Feng, D. Q.; Wu, Y.; Tsai, S. T.; Li, G.; Ray, C.; Yu, L. P. *J. Am. Chem. Soc.* **2009**, *131*, 7792−7799.
(29) Li, Y. F.; Cao, Y.; Gao, J.; Wang, D. L.; Yu, G.; Heeger, A. J. *Synth. Met.* **1999**, *99*, 243−248.
(30) Tamayo, A. B.; Walker, B.; Nguyen, T.-Q. *J. Phys. Chem. C* **2008**, *112*, 11545−11551.
(31) Walker, B.; Tomayo, A. B.; Dang, X. D.; Zalar, P.; Seo, J. H.; Garcia, A.; Tantiwiwat, M.; Nguyen, T.-Q. *Adv. Funct. Mater.* **2009**, *19*, 3063−3069.
(32) Matsuo, Y.; Sato, Y.; Niinomi, T.; Soga, I.; Tanaka, H.; Nakamura, E. *J. Am. Chem. Soc.* **2009**, *131*, 16048−16050.
(33) Yuan, M. C.; Chiu, M. Y.; Liu, S. P.; Chen, C. M.; Wei, K. H. *Macromolecules* **2010**, *43*, 6936−6938.
(34) Liang, Y. Y.; Wu, Y.; Feng, D. Q.; Tsai, S. T.; Son, H. J.; Li, G.; Yu, L. P. *J. Am. Chem. Soc.* **2009**, *131*, 56−57.
(35) Graham, K. R.; Mei, J. G.; Stalder, R.; Shim, J. W.; Cheun, H.; Steffy, F.; So, F.; Kippelen, B.; Reynolds, J. R. *ACS Appl. Mater. Interfaces* **2011**, *3*, 1210−1215.
(36) Yao, Y.; Hou, J. H.; Xu, Z.; Li, G.; Yang, Y. *Adv. Funct. Mater.* **2008**, *18*, 1783−1789.
(37) He, F.; Yu, L. P. *J. Phys. Chem. Lett.* **2011**, *2*, 3102−3113.
(38) Guo, X.; Cui, C. H.; Zhang, M. J.; Huo, L. J.; Huang, Y.; Hou, J. H.; Li, Y. F. *Energy Environ. Sci.* **2012**, *5*, 7943−7949.